Supporting Information

Green-antisolvent-regulated distribution of p-type self-doping enables tin perovskite solar cells with efficiency over 14%

Zhihao Zhang,[a]† Yuanfang Huang,[a]† Can Wang,[b] Yiting Jiang,[a] Jialun Jin,[a] Jianbin Xu,[b] Zicheng Li,[b] Zhenhuang Su,[e] Qin Zhou,[b] Jingwei Zhu,[a] Rui He,[a] Da Hou,[a] Huagui Lai,[d] Shengqiang Ren,[a*] Cong Chen,[a] Xingyu Gao,[e] Tingting Shi,[c] Walter Hu,[fg] Fan Fu,[d] Peng Gao,[b] Dewei Zhao [a*]

[a] College of Materials Science and Engineering & Engineering Research Center of Alternative Energy Materials & Devices, Ministry of Education, Sichuan University, Chengdu 610065, China

[b] CAS Key Laboratory of Design and Assembly of Functional Nanostructures, and Fujian Provincial Key Laboratory of Nanomaterials, Fujian Institute of Research on the Structure of Matter, Chinese Academy of Sciences Fuzhou, Fujian 350002, China

[c] Siyuan Laboratory, Guangzhou Key Laboratory of Vacuum Coating Technologies and New Energy Materials, Department of Physics, Jinan University, Guangzhou, 510632, China

[d] Laboratory for Thin Films and Photovoltaics, Empa-Swiss Federal Laboratories for Materials Science and Technology, Ueberlandstrasse 129, CH-8600 Duebendorf, Switzerland

[e] Shanghai Synchrotron Radiation Facility (SSRF), Zhangjiang Laboratory, Shanghai Advanced Research Institute, Chinese Academy of Sciences, Shanghai 201204, China

[f] State Key Lab of ASIC & System, Microelectronics Department, Fudan University, Shanghai 200433, China

[g] Precision Medicine Center, West China Hospital, Sichuan University, Chengdu 610041, China

† Authors contributed equally to this work.

E-mail: rensq@scu.edu.cn; dewei.zhao@scu.edu.cn; dewei_zhao@hotmail.com

Materials

All chemicals were purchased from Sigma Aldrich unless otherwise specified and used without further purification, including dimethyl sulfoxide (DMSO, 99.5%), N, N-dimethylformamide (DMF, 99.99%), chlorobenzene (CB, 99.99%), diethyl carbonate (DEC, 99%), tin (II) iodide (SnI_2, 99.99%), tin (II) fluorine (SnF_2, 99%), germanium (II) iodide (GeI_2, >99.8%, Sigma Aldrich), formamidinium iodide (FAI, >98%), ethylenediammonium diiodide ($EDAI_2$, >98.0%), and copper (Cu). Poly(3,4-ethylenedioxythiophene)polystyrene sulfonate (PEDOT: PSS, Clevious PVP AI 4083), BCP (99.9%), and C_{60} were purchased from Xi'an Polymer Light Technology.

Device fabrication

Sn-based perovskite solar cells were fabricated with the following structure: indium tin oxide (ITO)/PEDOT: PSS/$FASnI_3$/C_{60}/BCP/Cu. The glass substrates coated with ITO were cleaned with detergent, deionized water, and ethanol by ultrasonication for 30 min, respectively. Next, the dried ITO substrates were treated with ultraviolet ozone for 15 min. PEDOT: PSS was then spin-coated onto the ITO at 500 rpm for 10 s followed by 5000 rpm for 30 s with 1000 rpm/s acceleration rate and annealed at 180 ^{o}C for 20 min. Then the substrates were transferred into a glove box with a nitrogen atmosphere. The perovskite precursor solution was prepared by dissolving FAI, SnI_2, $EDAI_2$, SnF_2, and GeI_2 at a molar ratio of 0.99:1.0:0.01:0.1:0.05 in the mixed solvent of DMF and DMSO at a volume ratio of 4:1. For example, 1 mL perovskite precursor solution should be prepared by dissolving 170.25 mg FAI, 372.51 mg SnI_2, 3.16 mg $EDAI_2$, 15.67 mg SnF_2, and 16.32 mg GeI_2 into the mixed solvent of 800 μL DMF and 800 μL DMSO. The solutions should be stirring overnight before use. The perovskite precursor was filtered with 0.22 μm polytetrafluoroethylene before the spin-coating step. Next, 60 μL precursor solution was spin-coated onto the substrate at 5000 rpm for 50 s with 5000 rpm/s acceleration rate, and 300~600 μL (according to the area of substrates) CB or DEC was dripped onto the perovskite film at 15 s. Then the as-prepared films were annealed at 70 ^{o}C for 20 min. Afterward, C_{60} (25 nm), BCP (6 nm), and Cu (120 nm) were sequentially deposited via thermal evaporation in a vacuum chamber (base pressure, 5×10^{-4} Pa). The resultant active area of

0.0985 cm^2.

Time-drive steady-state absorption spectra

Time-drive steady-state absorption spectra were recorded in transmission mode on a Perkin Elmer Lambda 950 spectrophotometer using a perovskite deposited PEDOT:PSS/ITO/glass substrate.[1] Kinetics measurements were carried out as follows: PEDOT:PSS films were deposited on ITO/glass substrate and infiltrated with perovskites solution by spin-coating (the detailed parameters can be found in the part of device fabrication). Simulating the anti-solvent treatment procedure, the samples were then placed vertically in a standard cuvette of 10 mm path length using a Teflon holder. Corresponding antisolvents (CB or DEC) were then rapidly injected into the cuvette while the optical absorption at 430 nm was monitored.

Cross-sectional Kelvin probe force microscopy

The substrate was scribed on the film side, but out of the device region, then the glass was cleaved from the film side, without touching the device. It is better than cleaving from the backside, because cleaving from the backside would put a compressing force to the device films and damage the device cross-section we worked on.[2] The samples were cleaved in glove box and measured by KPFM. The cross-sectional kelvin probe force microscopy (KPFM) measurement was carried out by Bruker Nano Inc DI MultiMode 8 with 0.01~0.025 Ohm-cm Antimony doped Si probe at negative bias voltage. A frequency of ~75 KHz and a tip radius of ~20 nm were used to measure the potential images.

Derivation of charge density distribution from KPFM

The electric field distribution across the device cross section, $E(z)$, was calculated from the contact potential difference, $V(z)$, according to the equation:[3]

$$E(z) = -\frac{d}{dz}\left[V(z) - \frac{\Phi_{tip}(z)}{e}\right] = -\frac{d}{dz}V(z)$$

where $\Phi_{tip}(z)$ is the work function of the probe and e is the elementary charge. $\frac{\Phi_{tip}(z)}{e}$ is constant. The charge density distribution in a device, $\Delta\rho(z)$, is then given by:

$$\Delta\rho(z) = \epsilon_0\epsilon_r\frac{d}{dz}E(z)$$

where ϵ_0 and ϵ_r are the vacuum and relative permittivity, respectively. The data were smoothened with the Savitzky-Golay processing by a second-order polynomial regression and the same ratio of data points.[3]

Film characterizations

The X-ray diffraction (XRD) patterns were measured using a Shimazu XRD-6100 diffractometer with Cu-Kα radiation under operation conditions of 40 kV and 30 mA excitation. The top-view scanning electron microscopy (SEM) measurements were performed using a SUPRA 55, Zeiss, Germany, operated at an acceleration voltage of 5 kV. The Ultraviolet-visible (UV-vis) absorbance spectra of the perovskite films were measured using a Lambda 950 UV-Vis spectrophotometer (PerkinElmer). Ultraviolet Photoelectron Spectroscopy (UPS) was performed by PHI 5000 VersaProbe III with He I source (21.22 eV) under an applied negative bias of 9.0 V. The KPFM measurement for film surface was carried out by Bruker Nano Inc DI MultiMode 8 with 0.01~0.025 Ohm-cm Antimony doped Si probe at zero bias voltage. The time-of-flight secondary ion mass spectrometry (ToF-SIMS) depth profiles were acquired with a system (PHI nanoTOF II Time-of-Flight SIMS, Japan) via high mass resolution mode. An area of 80×80 μm^2 was analyzed using Bi_3^+ions with 30 keV energy and 0.30 pA current. The sputtering was performed using Cs^+ with 5 keV energy and 5 nA current within an area of 500×500 μm^2.

Device characterizations

The *J-V* curves were measured using Keysight B2901A source meter under AM1.5G (100 mW cm^{-2}) illumination in N_2-filled glove box with a scan rate of 50 mV s^{-1} and a dwell time of 100 ms. The light intensity was calibrated by silicon reference cells (SRC-00205, Enli Tech) with a solar simulator (SS-F5-3A, Enli Tech). The solar cells with a contact area of 0.0975 cm^2 were measured using a black shadow mask with an aperture area of 0.0576 cm^2. External quantum efficiency (EQE) was obtained on a computer-controlled quantum efficiency instrument (QE-R, Enlitech). The aging condition of oxygen environment for PSCs was achieved in a desiccator

(QHD260, ZISOdry) at room temperature (20 °C).

The Mott-Schottky measurements, thermal admittance spectrum (TAS), and drive-level capacitance profiling (DLCP) were carried out by an electrochemical workstation (Zennium Zahner, Germany). In the TAS measurement, the trap density of states (tDOS) is estimated from the angular frequency-dependent capacitance by: $N_T(E_\omega) = -\frac{V_{bi}\, dC\ \omega}{qWd\omega k_B T}$, where C is the capacitance, ω is the angular frequency, k is the Boltzmann constant, T is the temperature, V_{bi} and W represent the built-in potential and the depletion width extracted from the Mott-Schottky plot, respectively.[4,5] The applied angular frequency ω defines the energetic demarcation using: $E_\omega = k_B T ln\left(\frac{\omega_0}{\omega}\right)$, where ω_0 is the attempt-to-escape frequency and can be calculated from the frequency-dependent capacitance plot via the relaxation process.[6] The trap states below the energy demarcation are expected to capture or emit charge carriers with the given ω and contribute to the capacitance. In the DLCP measurement, the DC bias was set from 0 to 0.9 V, and a different AC bias (marked as dV, from 20 to 100 mV) was applied, with the AC frequency held as 10 kHz. The relationship between the capacitance and applied AC bias can be described by $\frac{C}{dV} = C_0 + C_1 dV + C_2 (dV)^2 + C_3 (dV)^3$. After recording the data, C_0 and C_1 can be obtained by fitting. The trap density (N_T) and the profiling distance (x) can be calculated by $N_T = -\frac{{C_0}^3}{2q\varepsilon\varepsilon_0 A^2 C_1}$ and $X = \varepsilon\varepsilon_0 A / C_0$, respectively. Here, q, ε, ε_0, and A represent the elementary charge, the relative permittivity of perovskite materials, vacuum permittivity, and active area, respectively.

DFT calculation

The details about the DFT calculation on the formation energies of vacancy defects in $FASnI_3$ under different chemical potential conditions can be found in Reference 7.

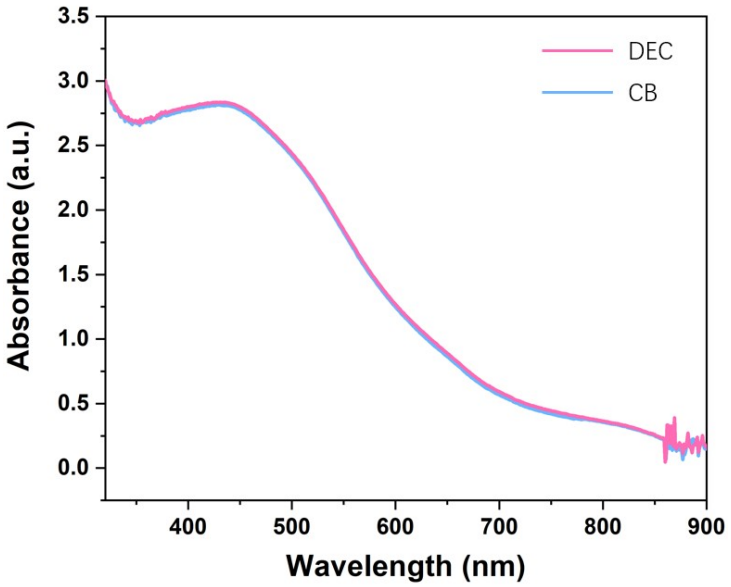

Fig. S1 UV-vis absorption spectra of the CB- and DEC-fabricated perovskite films after annealing.

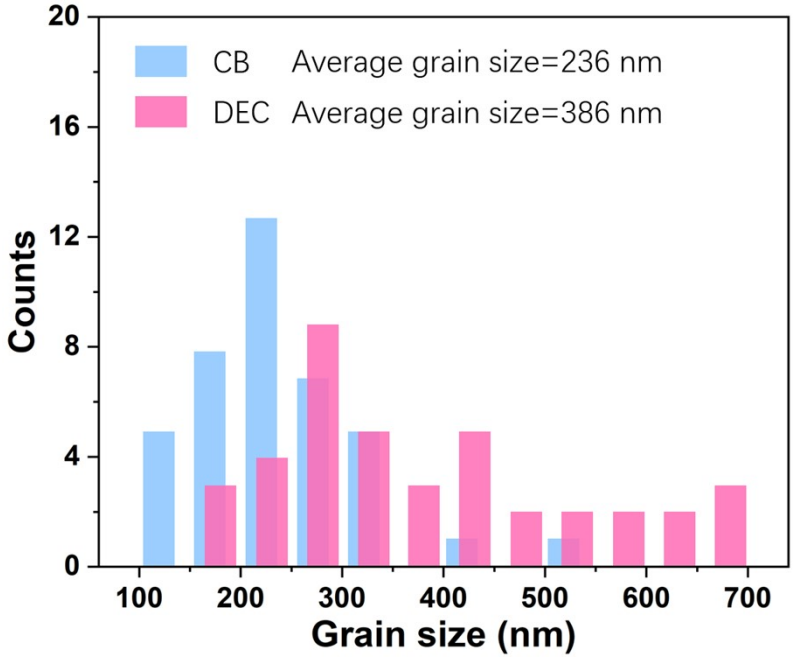

Fig. S2 Grain size distribution of CB- and DEC-fabricated films with their calculated average grain size.

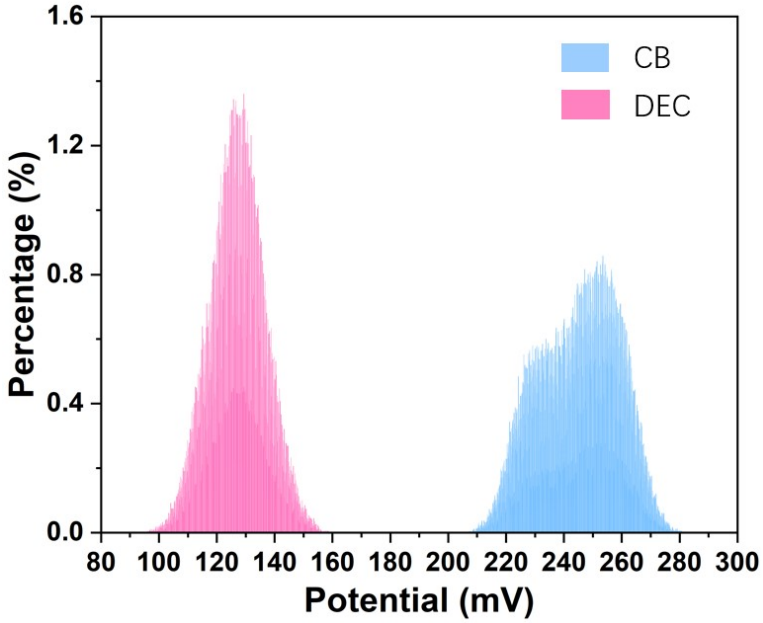

Fig. S3 Statistical distribution of the surface potential values extracted from top-view KPFM images.

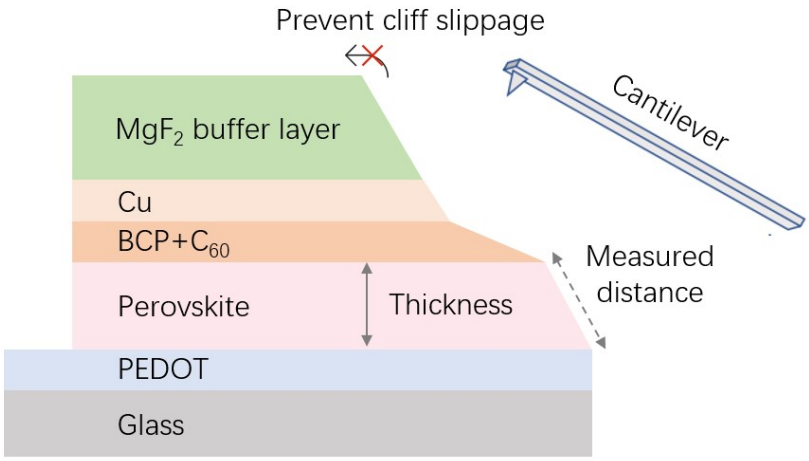

Fig. S4 Sschematic of cross-sectional KPFM measurement. Schematic illustrating the KPFM measurement setup and planar device structure of glass/ITO/PEDOT:PSS/$FASnI_3$/C_{60}/ BCP/Ag/MgF_2. The MgF_2 buffer layer prevents slippage of the cantilever tip at a "cliff". Often, the device cross-sections are not parallel, due to the uncontrollable nature of the mechanical cleaving process. Therefore, the measured distance may not represent the layer thickness.[3]

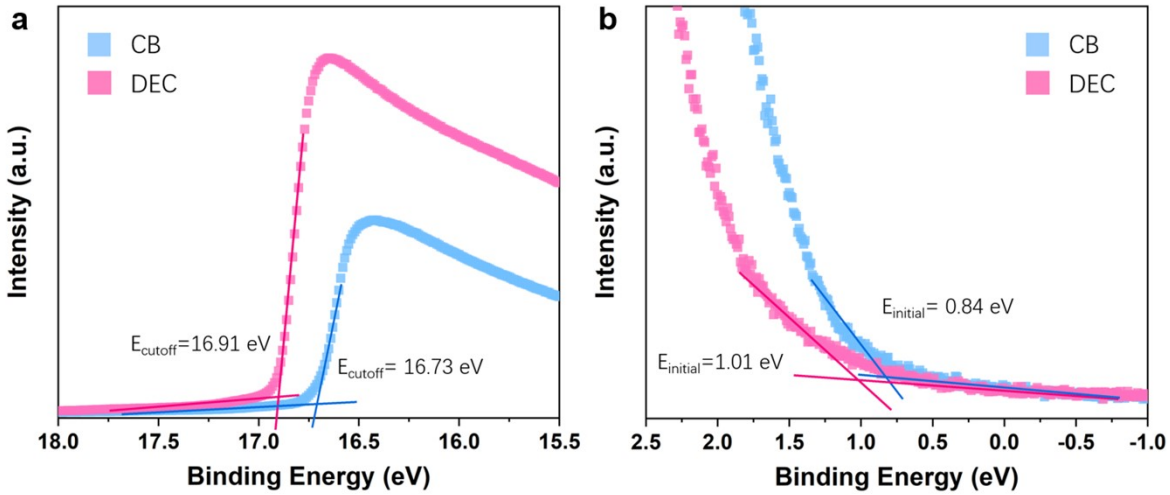

Fig. S5 UPS spectra of (a) the secondary edge region and (b) the valence band region (Fermi edge) of the CB- and DEC-fabricated films.

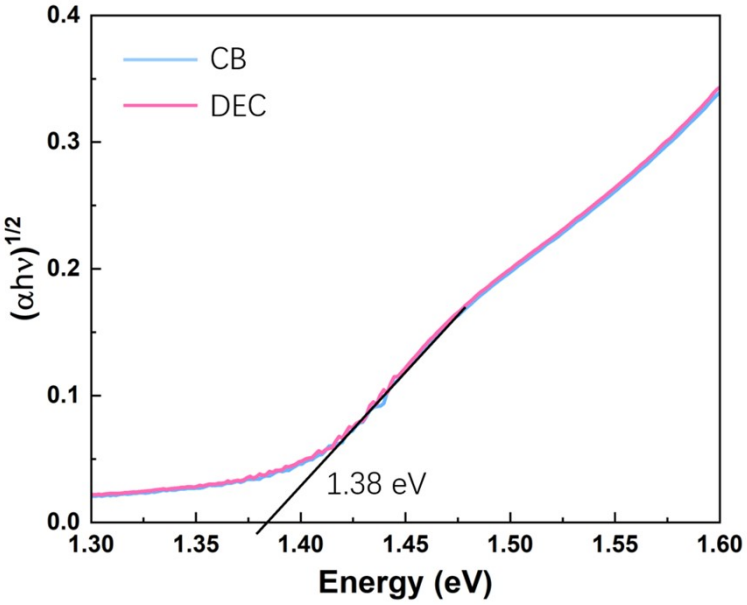

Fig. S6 Tauc plots of the CB- and DEC-fabricated films extracted from their corresponding absorption spectrum.

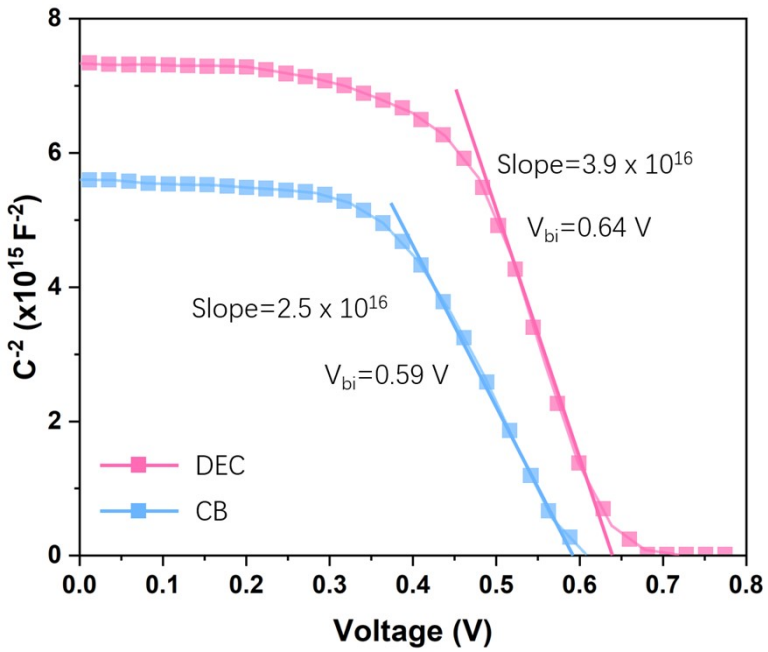

Fig. S7 Mott-Schottky plots for the CB- and DEC-fabricated PSCs.

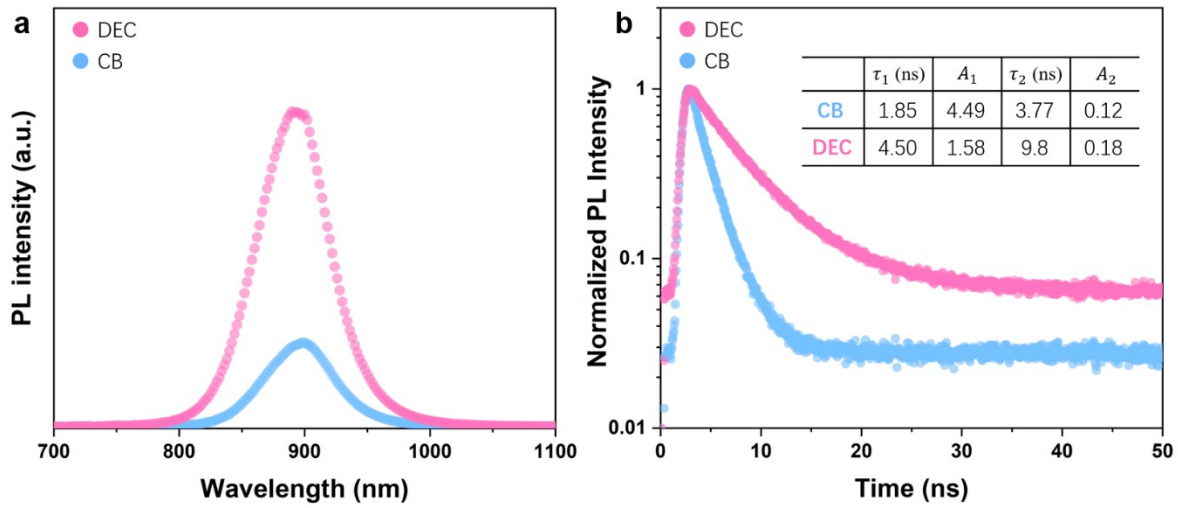

Fig. S8 (a) PL spectra and (b) TRPL decays of CB- and DEC-fabricated samples with a structure of glass/perovskite. The TRPL plot was fitted with a bi-exponential decay function defined as: $I = \gamma_0 + A_1 exp(-t/\tau_1) + A_2 exp(-t/\tau_2)$.

Table S1. Physicochemical properties of the solvents and antisolvents in this work.[1,8]

Solvents/ Antisolvents	Boiling point (°C)	Density (g/mL)	Dipole moment	Dielectric constant	DMF miscibility	DMSO miscibility	Film formation
DMSO	189	1.10	3.96 D	46.7	Yes	Yes	/
DMF	152	0.95	3.82 D	36.7	Yes	Yes	/
CB	131	1.1	1.69 D	5.62	Yes	Yes	Good
DEC	128	0.98	0.57 D	2.96	Yes	Yes	Good
Ethanol	78	0.79	1.66 D	25.7	Yes	Yes	Poor
Ethyl acetate	77	0.9	1.78 D	6.02	Yes	Yes	Poor
1-Butanol	117	0.81	1.64 D	17.5	Yes	Yes	Poor
Isopropanol	82.5	0.79	1.66 D	19.9	Yes	Yes	Poor

Table S2. Metrics for drawing the energy levels extracted from the UPS results.

Sample	E_{cutoff} (eV)	E_{intial} (eV)	W_F (eV)	VBM (eV)	CBM (eV)
CB	16.73	0.84	4.49	-5.32	-3.94
DEC	16.91	1.01	4.31	-5.33	-3.95

Table S3 Summary on photovoltaic parameters of the champion CB- and DEC- fabricated PSCs under reverse and forward scan. The hysteresis index (HI) is calculated using the values of average PCE by equation $HI = (PCE_{RS} - PCE_{FS})/PCE_{RS}$.

Sample	Scanning direction	J_{SC} (mA cm^{-2})	V_{OC} (V)	FF (%)	PCE (%)	HI
CB	reverse	23.2	0.72	72.5	12.1	0.017
	forward	22.7	0.72	72.9	11.9	
DEC	reverse	24.2	0.80	73.5	14.2	0
	forward	24.1	0.80	73.9	14.2	

References

1 S. Paek, P. Schouwink, E. N. Athanasopoulou, K. T. Cho, G. Grancini, Y. Lee, Y. Zhang, F. Stellacci, M. K. Nazeeruddin and P. Gao, *Chem. Mater.*, 2017, **29**, 3490–3498.

2 C. Xiao, C. Wang, W. Ke, B. P. Gorman, J. Ye, C. S. Jiang, Y. Yan and M. M. Al-Jassim, *ACS Appl. Mater. Interfaces*, 2017, **9**, 38373–38380.

3 S. Tan, T. Huang, I. Yavuz, R. Wang, T. W. Yoon, M. Xu, Q. Xing, K. Park, D. K. Lee, C. H. Chen, R. Zheng, T. Yoon, Y. Zhao, H. C. Wang, D. Meng, J. Xue, Y. J. Song, X. Pan, N. G. Park, J. W. Lee and Y. Yang, *Nature*, 2022, **605**, 268–273.

4 S. Khelifi, K. Decock, J. Lauwaert, H. Vrielinck, D. Spoltore, F. Piersimoni, J. Manca, A. Belghachi and M. Burgelman, *J. Appl. Phys.*, 2011, **110**, 094509..

5 F. Paquin, J. Rivnay, A. Salleo, N. Stingelin and C. Silva, *Energy Environ. Sci.*, 2015, **3**, 10715–10722.

6 J.-W. W. Lee, D.-H. H. Kim, H.-S. S. Kim, S.-W. W. Seo, S. M. Cho and N.-G. G. Park, *Adv. Energy Mater.*, 2015, **5**, 1501310.

7 T. Shi, H. S. Zhang, W. Meng, Q. Teng, M. Liu, X. Yang, Y. Yan, H. L. Yip and Y. J. Zhao, *J. Mater. Chem. A*, 2017, **5**, 15124–15129.

8 R. Vidal, J. A. Alberola-Borràs, S. N. Habisreutinger, J. L. Gimeno-Molina, D. T. Moore, T. H. Schloemer, I. Mora-Seró, J. J. Berry and J. M. Luther, *Nat. Sustain.*, 2021, **4**, 277–285.